EurJOC European Journal of Organic Chemistry

FULL PAPER

DOI: 10.1002/ejoc.201300207

Molecular Tweezers with Freely Rotating Linker and Porphyrin Moieties

Rhys B. Murphy,[a] Duc-Truc Pham,[b] Stephen F. Lincoln,[b] and Martin R. Johnston*[a]

Keywords: Supramolecular chemistry / Molecular recognition / Porphyrinoids / Sandwich complexes / Metalloporphyrins / Cycloaddition

Molecular tweezers were synthesised by using a microwave accelerated alkene plus cyclobutane epoxide reaction between norbornyl appended porphyrin moieties and a diepoxide functionalised phenyl diimide spacer. The tweezers contain several rotational degrees of freedom; about the porphyrin with respect to the norbornyl linker, and between the two norbornyl backbone sections. The ability of Zn^{II} metallated tweezer **1** to complex 1,4-diazabicyclo[2.2.2]-octane (DABCO) was studied by UV/Vis and ^1H NMR spectroscopy and multivariate global spectral analysis. The system was found to form a strong 1:1 intramolecular complex (**1**:DABCO) with an association constant of $K_{11} = 8.1 \times 10^7\ M^{-1}$, transforming to a 1:2 open complex [**1**:$(DABCO)_2$] with $K_{12} = 2.7 \times 10^9\ M^{-2}$ at high concentrations of DABCO.

Introduction

Molecular tweezers have been the focus of much research over the last several decades and continue to be actively pursued today, with several large reviews being recently published.[1] A plethora of architectures have been synthesised which accommodate guests such as aromatic compounds,[2] anions,[3] cations,[4] fullerenes[5] and amines.[3,5a,6] This versatility in design, structure and function makes molecular tweezers suitable candidates for the fabrication of nanoscale molecular devices.[1a,1c] Consequently, molecular tweezers are beginning to find applications in targeted drug delivery and controlled release,[2c] and in the determination of enantiomeric purity or absolute configuration of chiral guest compounds.[7]

Metalloporphyrins are ideal components of molecular tweezers because the metal centre coordinates axially with diamine guests, generating sandwich complexes with large association constants.[1b,6g,8] There has been significant work on bis-porphyrin tweezers and capsules,[3,5a,6] including those containing bridged polycyclic backbones.[9] These polycyclic backbones are characterised by a high degree of rigidity when they do not contain semi-flexible components such as non bridged cyclohexane(ene) rings or fused aromatic rings.[9c,10]

We report herein our latest molecular tweezer design, in which we have opted for linkages that introduce rotational degrees of freedom about single bonds. Bis-porphyrin hosts containing linkers that allow defined changes in both interporphyrin distance and angle have been reported.[11] However, this has little effect on the strength of complex formation in systems of varying degrees of preorganisation[6i,6k–6m,9a,9b,12] relative to more constrained hosts. We have used UV/Vis and NMR spectroscopy to follow the interaction of Zn^{II} metallated tweezer **1** with diamine guest DABCO and determined the association constant for this complexation by using multivariate global spectral analysis (Figure 1).

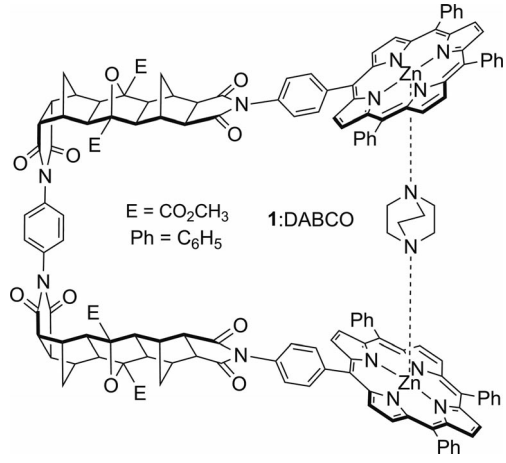

Figure 1. Molecular tweezer complex, **1**:DABCO.

Results and Discussion

Synthesis

The synthesis of molecular tweezer **1** began with condensation of *exo*-anhydride **2**[13] with aminoporphyrin **3**,[14]

[a] Flinders Centre for NanoScale Science & Technology, School of Chemical and Physical Sciences, Flinders University, Bedford Park, Adelaide, Australia
Fax: +61-8-8201-2905
E-mail: martin.johnston@flinders.edu.au
Homepage: http://www.flinders.edu.au/people/martin.johnston
[b] School of Chemistry and Physics, The University of Adelaide, Adelaide, Australia

Supporting information for this article is available on the WWW under http://dx.doi.org/10.1002/ejoc.201300207.

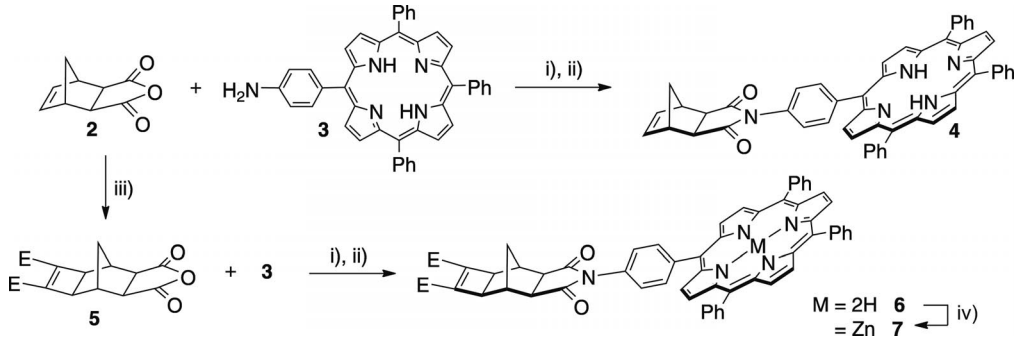

Scheme 1. (i) $CHCl_3$, reflux, overnight, Ar deoxygenated; (ii) $NaOAc/Ac_2O$, 80 °C, overnight, **4** 72%, **6** 84%; (iii) DMAD (2 equiv.), $[RuH_2(CO)(PPh_3)_3]$ (5 mol-%), toluene, 100 °C, 3 d, 67%; (iv) $Zn(OAc)_2/MeOH/CHCl_3$, reflux, 30 min, 95%.

generating porphyrin block **4** (Scheme 1). Product **4** was characterised with NMR spectroscopy and revealed resonances typical for porphyrin and norbornyl moieties. Anhydride **2** was also reacted with dimethyl acetylenedicarboxylate (DMAD) using the Mitsudo reaction,[15] which is a ruthenium catalysed[16] [2+2] cycloaddition, to yield **5**. Subsequent reaction with aminoporphyrin **3** gave compound **6**, which was metallated in the normal manner[17] to give **7**.[18] This latter material was used in UV/Vis studies as the monomeric porphyrin component of tweezer **1**, which was the subject of UV/Vis complexation equilibrium studies.

Joining two molecules of **4** together was achieved by using linker molecule **12** (Scheme 2). Compound **12** was synthesised from *endo*-anhydride **8**,[19] which was appended with a methyl ester substituted cyclobutene ring by Mitsudo reaction with DMAD, to give **9**. In contrast to previous reports,[20] we obtained good yields of **9** in our reactions. Two equivalents of **9** were subsequently ring opened at the anhydride functionality by *p*-phenylenediamine (**10**) to generate the diamic acid (not shown), which upon ring closing yielded phenyl diimide linker **11**. The conversion of **11** into diepoxide **12** was achieved through a nucleophilic epoxidation[21] by using anhydrous *tert*-butyl hydroperoxide in toluene[22]/potassium *tert*-butoxide.

Coupling of **4** and **12** (used as a mixture with **11**) to give free base tweezer **13** was achieved by the alkene plus cyclobutane epoxide (ACE) reaction (Scheme 2), which generates *exo*-fused bridged polycyclic backbones through thermal ring opening of the epoxide to a 1,3-dipole, followed by 1,3-dipolar [3+2] cycloaddition reaction with a norbornene dipolarophile.[21] Conventionally, this reaction takes place in a sealed tube under medium to forcing reaction conditions, at temperatures as high as 170 °C[9b] for as long as 90 h.[9a] However, with the recent development of microwave accelerated ACE reactions,[23] reaction times are reported to be much shorter (10 to 60 min) with little degradation. The microwave accelerated ACE reaction was found to lend itself to our substrates, giving **13** in 38% yield.

Free base tweezer **13** was identified by several features in the NMR spectra characteristic of ACE reactions. The resonance at δ = 90 ppm in the ^{13}C NMR spectrum is observed in similar polycyclic systems[10e] and is assigned to the bridgehead carbon atoms in the newly formed methyl ester substituted oxanorbornane.[10e] In the ^1H NMR spec-

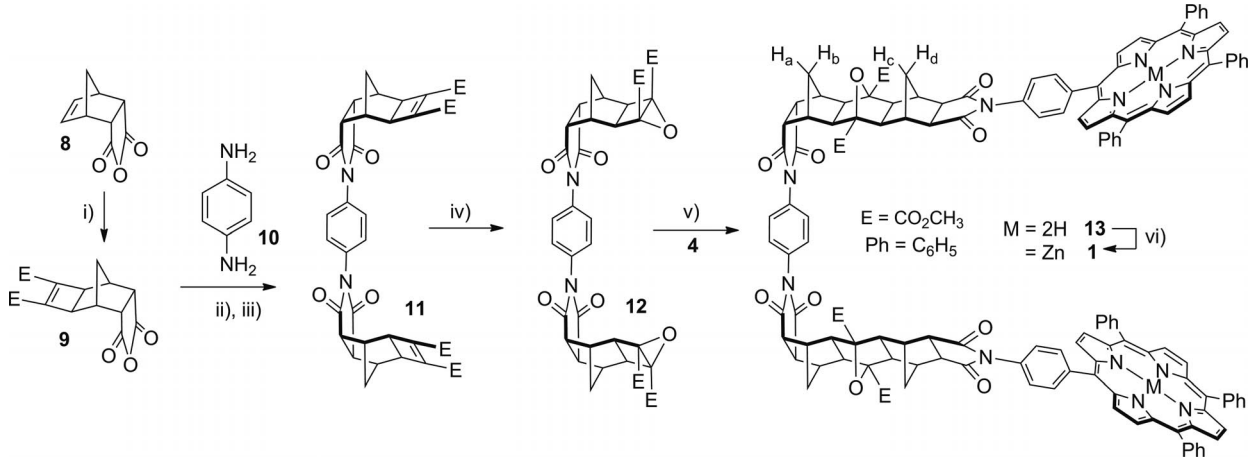

Scheme 2. (i) DMAD (2 equiv.), $[RuH_2(CO)(PPh_3)_3]$ (5 mol-%), toluene, 100 °C, 3 d, 77%; (ii) *p*-phenylenediamine (**10**, 0.5 equiv.), Ar deoxygenated, dry DMF, 80 °C, 3 d; (iii) $NaOAc/Ac_2O$, 80 °C, 3 d, 25%; (iv) anhydrous *t*BuOOH in toluene (3.3 M, 2.5 equiv.), dry CH_2Cl_2, 0 °C, 10 min, *t*BuOK (1 equiv.), room temp., 3.5 h, 28%; (v) **4** (2 equiv.), dry THF, microwave 80–220 W, 14–20 bar, 180 °C, 2 h, 38%; (vi) $Zn(OAc)_2/MeOH/CHCl_3$, reflux, 30 min, 95%.

trum, a small downfield shift was observed for the methyl ester resonance,[23] along with the disappearance of the norbornene proton resonance from **4** at δ = 6.45 ppm. Furthermore, the ^{1}H COSY spectrum reveals two separate spin systems for the *endo*- and *exo*-components of the backbone within **13**. The methylene bridge protons H_a/H_b and H_c/H_d (Scheme 2) appear at significantly different chemical shifts, characteristic of steric compression by oxygen in these systems,[20] and confirms the formation of a linear ACE product.[20] These resonances occur at chemical shifts of δ = 1.38/2.75 and 1.22/2.55 ppm, however the absence of nOe signals prevented their exact assignment as either H_a/H_b or H_c/H_d. Within the aromatic region of the ^{1}H NMR spectrum of **13**, there is some evidence of splitting within the *meso*-phenyl resonances, indicating facial differentiation and interaction of the two porphyrins within the tweezer at millimolar (NMR) concentrations. HRMS further confirmed the identity of **13**: calcd. $[M + H]^+$ 2267.7813; found 2267.7854.

Zinc(II) metallation of **13** under standard conditions[17] to give target tweezer **1** was characterised by loss of the porphyrin inner pyrrole proton resonance at δ = –2.81 ppm, and was further confirmed by HRMS: calcd. $[M + H]^+$ 2391.6094; found 2391.6044. Although changes to the UV/Vis spectrum of porphyrins are typically observed upon metallation, in this case there was no significant shift in the Soret band, with only changes to the Q-bands being observed. Dilution of a chloroform solution of **1** (10^{-5} to 10^{-7} M) resulted in only minor changes to the peak width, indicating that there was no significant aggregation of the tweezer. In addition, at NMR concentrations (19 to 2.3 mM), only minor (< 0.1 ppm) shifts were observed in the resonances for **1**, again indicating no significant aggregation.

Host-Guest Titrations with DABCO

The interaction between Zn^{II} tweezer **1** and the diamino ligand DABCO was examined by UV/Vis and NMR spectroscopy. In line with other bis-porphyrin host systems reported in the literature,[6e–6i,11] host **1** is in rapid equilibrium between a variety of conformations, the extremes of which are *syn*- and *anti*-. These can form various complexes in solution, all of which are in equilibrium. These possibilities are outlined schematically in Figure 2 and reveal the possibility of 1:1, $\{K_{11} = [\mathbf{1}{:}DABCO]/([\mathbf{1}][DABCO])\}$, 1:2 $\{K_{12} = [\mathbf{1}{:}(DABCO)_2]/([\mathbf{1}][DABCO]^2)\}$, 2:1 $\{K_{21} = [\mathbf{1}_2{:}DABCO]/([\mathbf{1}]^2[DABCO])\}$ and 2:2 $\{K_{22} = [\mathbf{1}_2{:}(DABCO)_2]/([\mathbf{1}]^2[DABCO]^2)\}$ stoichiometries.

UV/Vis Spectroscopy

Prior to analysis of the bis-porphyrin system **1**, we studied the complexation of mono-porphyrin compound **7**. Dilution of a chloroform solution of **7** resulted in only minor changes to the peak width, indicating that there was no significant aggregation of the mono-porphyrin. Titration of a solution of monodentate quinuclidine (1-azabicyclo[2.2.2]octane) **14** to a solution of **7** resulted in a red shift of the Soret band from 419.3 nm in **7** to 430.6 nm, indicating the formation of **7**:**14**. The UV/Vis titration data was analysed by using multivariate global spectral analysis (HypSpec, Protonic Software[24]), and the microscopic binding constant K_{11} was determined to be 2.5×10^5 M^{-1} in $CHCl_3$. This association constant is similar to the value observed for other mono-porphyrin quinuclidine complexes in the literature,[6g] thus it can be concluded that the norbornyl backbone has little influence on the complexation ability of the metalloporphyrin.

The UV/Vis spectra of mono-porphyrin **7** and bis-porphyrin tweezer **1** are almost identical in peak shape, with Soret peak band-widths at half height of 10 and 11 nm, respectively. This is indicative of the absence of interactions between the porphyrins in **1**[6n,25] at UV/Vis concentrations (10^{-5} to 10^{-7} M), and suggests that the porphyrin units are able to undergo rapid rotation about the single bond between the imide and porphyrin moiety and/or the linking aromatic unit between the arms of the tweezer at these concentrations.

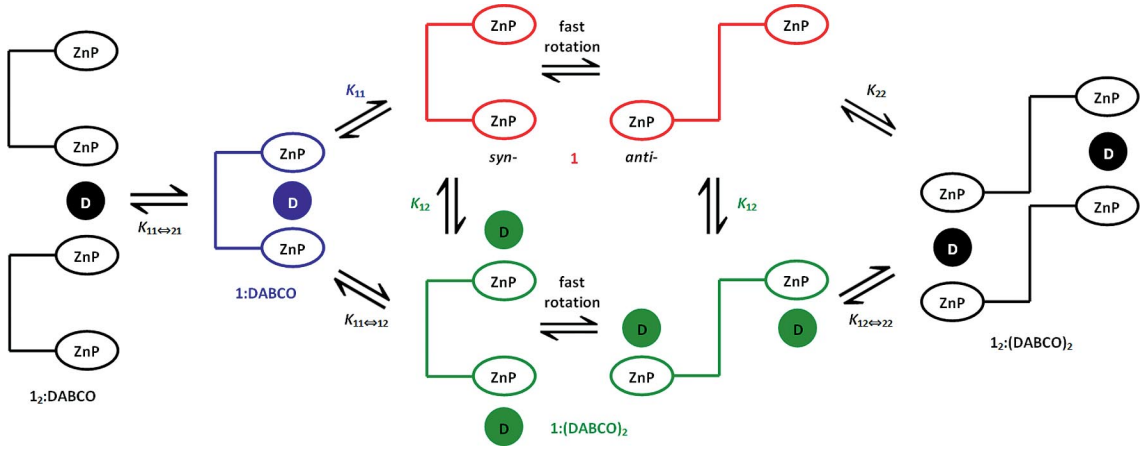

Figure 2. Schematic representation of the various equilibria between **1** and DABCO.

Titration of a solution of DABCO into a solution of bis-porphyrin tweezer **1** resulted in a red shift of the UV/Vis spectrum (Figure 3), with the Soret maximum moving from 419.5 to 423.4 nm, and is characteristic of a bis-porphyrin DABCO sandwich complex.[6g,6h] The red shift was essentially complete after the addition of slightly greater than one equivalent of DABCO. A clear isosbestic point was observed, which suggests that complexation proceeds between two well-defined species in solution without generating an intermediate species.[6e,6g,6h,6l] The sandwich complex is stable in the presence of an excess of DABCO (approximately 5000 equiv.), after which it is slowly converted most likely to an open **1**:$(DABCO)_2$ complex, in which DABCO is bound to each porphyrin singly rather than as a sandwich. This transition is only half complete by the addition of 45000 equiv., and only after the addition of 200000 equiv. does this become the dominant species in solution, with a Soret maximum of 429.4 nm. This is characteristic of simple mono-porphyrin DABCO complexes,[6g,6h] and is similar to that observed for simple mono-porphyrin quinuclidine complex **7**:**14**.

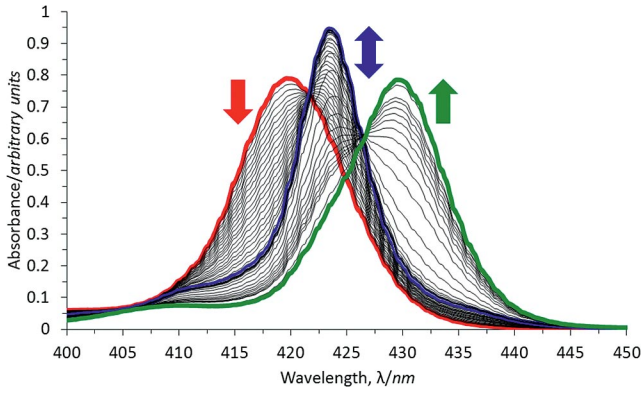

Figure 3. UV/Vis titration of **1** with DABCO in chloroform [red line **1**, blue line **1**:DABCO, green line **1**:$(DABCO)_2$].

Shown in Figure 4 (a and b) are speciation diagrams for the UV/Vis titration data that have been separated out into 0–2 equiv. DABCO and 0–200000 equiv. DABCO. Clearly visible is the initial formation of the 1:1 complex between **1** and DABCO (**1**:DABCO), and its conversion into the 1:2 complex [**1**:$(DABCO)_2$] as more equivalents of DABCO are added to the solution. Given the possible complexation geometries shown in Figure 2, we attempted to fit the UV/Vis titration data to account for the formation of 2:2 and 2:1 complexation stoichiometries, $\mathbf{1}_2$:$(DABCO)_2$ (K_{22}) and $\mathbf{1}_2$:DABCO (K_{21}), respectively. However, the data could not be fitted to these species, suggesting that the ternary intermolecular complexes $\mathbf{1}_2$:$(DABCO)_2$ and $\mathbf{1}_2$:DABCO are not formed to any appreciable extent at UV/Vis concentrations (10^{-5} to 10^{-7} M). The UV/Vis titration data gave an excellent fit for a 1:1 plus 1:2 binding model, giving K_{11} = 8.1×10^7 M^{-1} and K_{12} = 2.7×10^9 M^{-2} in $CHCl_3$, and were assigned to intramolecular **1**:DABCO and open **1**:$(DABCO)_2$, respectively (Figure 2). The best fit of the algorithm for the formation of **1**:DABCO and **1**:$(DABCO)_2$ to the titration data is shown in Figure 4 (c and d). The K_{11} obtained for **1**:DABCO is over two orders of magnitude larger than **7**:**14**, and this enhancement is indicative of a bis-porphyrin DABCO sandwich complex.[6i,6k,6m] A summary of the UV/Vis data is provided in Table 1.

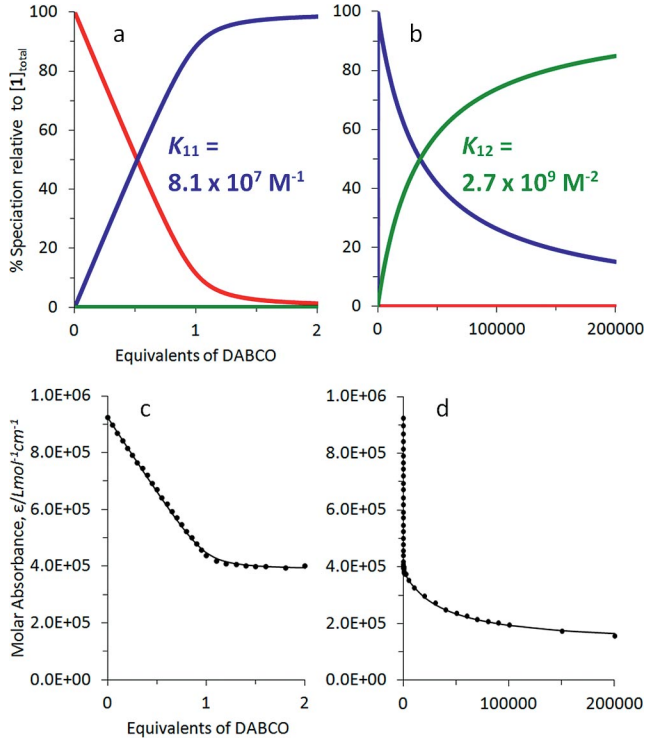

Figure 4. Speciation diagram of **1** with DABCO (HypSpec, HySS2009) for (a) 0–2 equiv.; (b) 0–200000 equiv. [red line **1**, blue line **1**:DABCO, green line **1**:$(DABCO)_2$]; (c) Best fit (black line) of the algorithm for equilibria between **1**, DABCO, **1**:DABCO and **1**:$(DABCO)_2$ to the titration data (black circles) for 0–2 equiv. of DABCO; (d) 0–200000 equiv. of DABCO.

Table 1. Summary of UV/Vis data in chloroform.

Species	**7**	**7**:**14**	**1**	**1**:DABCO	**1**:$(DABCO)_2$
λ_{max} (nm)	419.3	430.6	419.5	423.4	429.4
K_a		2.5×10^5 M^{-1}		8.1×10^7 M^{-1}	2.7×10^9 M^{-2}
Width[a] (nm)	10		11		

[a] Peak band width measured at half height.

Although the porphyrins in **1** can freely rotate about the bonds adjacent to the phenyl group, and either half of **1** may rotate about the bond to the central phenyl diimide group, the large association constants observed for **1**:DABCO and **1**:$(DABCO)_2$ support the observations by others[6l,6m,9a,12b] that systems need only be moderately pre-organized for large association constants to arise. Such rotational freedom has been found to enhance host responsiveness in catalysing the rate acceleration of a hetero-Diels–Alder reaction[12a] and in the mechanical twisting of a guest by a light-powered molecular pedal.[6a]

^{1}H NMR Spectroscopic Studies

^{1}H NMR spectroscopy has been extensively used to characterise supramolecular complexes in solution because it is able to give information on chemical environments of nuclei as well as on speciation. We sought to characterise **1**:DABCO and **1**:(DABCO)$_2$ through ^{1}H NMR titration of **1** with DABCO in $CDCl_3$. At 20 °C, the β-pyrrole signals for uncomplexed **1** are at δ = 8.94 ppm (Figure 5, a). The addition of 0.5 equiv. of DABCO resulted in a broadening of the porphyrin β-pyrrole resonance and the appearance of a second β-pyrrole signal for the complex at δ = 8.54 ppm, most likely **1**:DABCO. This upfield shift is typical of β-pyrrole protons in a bis-porphyrin DABCO sandwich complex and results from shielding by opposing ring currents of two porphyrin aromatic systems in close proximity.[6g,6h,26] The species are in slow exchange on the NMR timescale at ambient temperature up to 0.9 equiv. of DABCO, and the β-pyrrole complex signal increases at the expense of uncomplexed **1**. Addition of 5 equiv. of DABCO causes the β-pyrrole resonance to shift downfield as increasing proportions of **1**:(DABCO)$_2$ form in fast exchange.

Further understanding of the complexation of DABCO by **1** is gained from the DABCO methylene resonance (Figure 5, b). For the addition of up to 0.9 equiv. of DABCO, a sharp singlet was observed at –4.89 ppm (Figure 5, b), and shows the expected integration for each addition of DABCO. This large upfield shift is typical of DABCO methylene protons in a bis-porphyrin DABCO sandwich complex, and again results from shielding by opposing ring currents of two porphyrin aromatic systems in close proximity.[6d,6f–6h,26–27]

At one equivalent of DABCO, the **1**:DABCO resonance is broader, consistent with chemical exchange occurring with another species at a fast exchange rate on the NMR timescale at 20 °C. Slowing the exchange rate by lowering the temperature to –50 °C revealed a second broad signal at –3.0 ppm (shown by asterisk Figure 5, b), which is characteristic of the α methylene protons of DABCO bound to a single porphyrin,[6e–6g] and most likely corresponds to the destruction of the intramolecular **1**:DABCO complex to the open **1**:(DABCO)$_2$ complex. Furthermore at –50 °C and one equivalent of DABCO, two weak bis-porphyrin DABCO sandwich complex signals are observed in addition to the main signal at –5 ppm (shown by arrows in Figure 5, b). These are attributed to the formation of small amounts of ternary intermolecular complexes other than intramolecular **1**:DABCO, such as **1**$_2$:(DABCO)$_2$ and **1**$_2$:DABCO. When 1.25 equiv. of DABCO are added at –50 °C, the broadened open **1**:(DABCO)$_2$ resonance increases in area whereas the **1**:DABCO resonance broadens as its concentration diminishes, and exchange between the two complexes increases.

In addition, at –50 °C and less than one equivalent of DABCO, differentiation of the *meso*-phenyl proton resonances depending on their facial orientation within the complex was observed (not shown). No further desymmetrisation of the spectrum was observed to –90 °C for approximately 0.25 equiv. of DABCO in CD_2Cl_2.[28] This indicated that axial ligand rotation of DABCO about the Zn–Zn axis of the bis-porphyrin sandwich was rapid on the NMR timescale at this temperature.[29] NOESY of this same solution at –60 °C revealed dipolar connectivity between the DABCO signal and both the β-pyrrole complex signal and several *meso*-phenyl complex signals.[30]

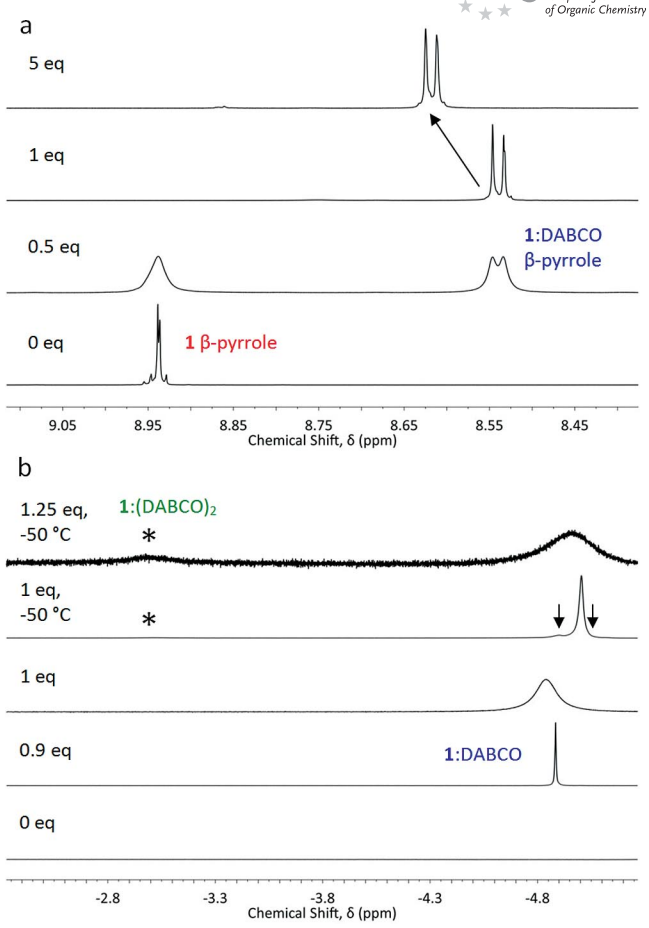

Figure 5. Selected ^{1}H NMR spectra with various equivalents of DABCO. (a) β-Pyrrole region; (b) complexed DABCO region. Asterixes show DABCO resonances within the **1**:(DABCO)$_2$ complex. Arrows identify the minor amount of **1**$_2$:(DABCO)$_2$ and **1**$_2$:DABCO complexes formed in addition to the main complex **1**:DABCO.

To further investigate the composition of the complex formed between **1** and DABCO at millimolar concentrations, a simulated NMR speciation diagram was generated by using association constants K_{11} and K_{12} determined from the UV/Vis titrations and analysed relative to experimental NMR titration data.[6g,6h] When < 1 equiv. of DABCO is added, the system is in slow exchange on the NMR timescale and the relative amounts of free and complexed **1** can be determined from the integration of the β-pyrrole resonances. Figure 6 shows the simulated NMR speciation diagram for 1:1 (**1**:DABCO) plus 1:2 [**1**:(DABCO)$_2$] species (HySS2009, Protonic Software[24]) and the experimentally determined NMR speciation for the slow exchange region of the titration. The excellent correlation between the simulated and experimental speciation in

the 1:1 region of the plot confirms the formation of intramolecular complex **1**:DABCO as the dominant species at both UV/Vis and NMR concentrations.

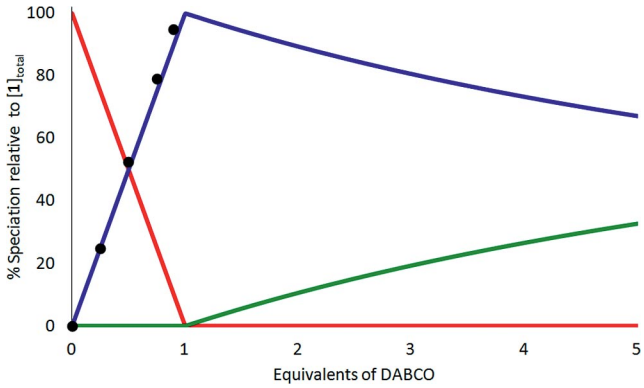

Figure 6. Simulated NMR speciation diagram [red line **1**, blue line **1**:DABCO, green line **1**:$(DABCO)_2$] generated from UV/Vis determined association constants K_{11} and K_{12}, and experimental NMR speciation (black circles) for the slow exchange region of the NMR titration (< 1 equiv. of DABCO).

Molecular modelling (Spartan '10, Wavefunction, Inc.[31]) was undertaken to determine the equilibrium geometry of the **1**:DABCO complex. The semi-empirical (AM1) calculation is shown in Figure 7. The porphyrin moieties are rotated somewhat relative to the idealised representation in Figure 1. Rotation is also observed between the two norbornyl arms of the tweezer about the central phenyl diimide group. However, there does not appear to be any strain within the complex and this supports the high association constant that has been determined.

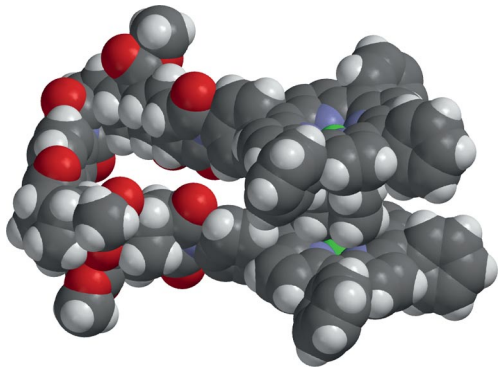

Figure 7. Semi-empirical (AM1) molecular modelling of the **1**:DABCO complex.

Conclusions

We have designed and successfully synthesised a bis-porphyrin containing molecular tweezer in which the porphyrin units are able to rotate freely with respect to the norbornyl backbone as well as the central linking phenyl diimide unit. The tweezer forms a strong intramolecular 1:1 complex with DABCO (**1**:DABCO), moving to an open 1:2 complex [**1**:$(DABCO)_2$] at high concentrations of DABCO, with association constants of $K_{11} = 8.1 \times 10^7$ M^{-1} and $K_{12} = 2.7 \times 10^9$ M^{-2}, respectively. The same complexation stoichiometry was found to occur at the different concentrations employed in the UV/Vis and NMR experiments.

Our current synthetic efforts are directed towards analogues of **1** that contain a sterically bulky 2,3,5,6-tetramethyl-substituted phenyl linker. This system is expected to exhibit restricted rotation about the central phenyl diimide linking unit and will allow us to isolate the *syn*- and *anti*-conformations as separate species. The complexation with ligands such as DABCO should then allow for the formation of 1:1 and 2:2 species separately.

Experimental Section

General Methods: NMR spectra were recorded with a Bruker UltraShield Avance III 400 MHz or 600 MHz NMR Spectrometer running the TopSpin 2.1 software package at 299 K and 293 K, respectively. $CDCl_3$ was deacidified by passing it through neutral activated aluminium oxide 70–290 mesh (Scharlau, activity degree 1, grain size 0.05–0.2 mm) and stored over silver foil/molecular sieves. NMR host-guest titrations were carried out at constant host concentrations of ≈ 10^{-3} M in $CDCl_3$.

Microwave reactions were performed in a CEM Discover S-Class microwave in reaction vessels (10 mL) loaded with combined starting materials (0.25g) in solvent (no more than 2 mL). The microwave was operated in variable power (dynamic) mode with the following parameters: power 300 W, pressure 20 bar, temperature 180 °C, stirring high, air/nitrogen cooling off. Ramp time to 180 °C was 30 min, with the pressure reaching 16.5 bar. The sample was held at this temperature for a further 60 min, automatically modulating the power between 80–220 W, with the pressure tapering to 14 bar.

UV/Vis spectra were recorded with a Cary 50 instrument at 20 °C in a Starna Type 21 SX 1 cm^2 quartz cuvette with the following parameters: average time 0.05 s, data interval 0.15 nm, scan rate 180 nm/min, wavelength range 300–700 nm, baseline correction against chloroform. All UV/Vis spectra were recorded in dry $CHCl_3$, prepared by heating to reflux over P_2O_5/distillation,[32] and deacidified as above. UV/Vis host-guest titrations were carried out at constant host concentrations of ca. 10^{-6}–10^{-7} M in $CHCl_3$.

All samples for host-guest titrations were weighed with either a Shimadzu AUW220D or a AandD GR-202 five decimal point balance. Volumetric glassware (A) was used for volumes ≥ 1 mL, and SGE and Hamilton gas-tight microlitre syringes for volumes 10–500 μL. Association constants and speciation diagrams were calculated from the UV/Vis titration data using the HypSpec and HySS2009 software packages[24] over 400–450 nm. Errors were estimated to be 10%.

High-resolution mass spectrometry measurements of tweezers **13** and **1** were recorded with an Agilent 6220 TOF mass spectrometer fitted with a dual ESI source by using a fragmentor voltage of 300 V. All other compounds were recorded with a Waters Synapt HDMS; electrospray, positive ion with lockspray.

Molecular modelling of equilibrium geometry was calculated at a semi-empirical (AM1) level with the Spartan '10 software package.[31]

Melting points were measured with a Barloworld Scientific SMP10 melting point apparatus.

Dry tetrahydrofuran (THF) was freshly distilled from sodium/benzophenone, dry CH_2Cl_2 freshly distilled from CaH_2, and dry

dimethylformamide (DMF) distilled under reduced pressure onto fresh molecular sieves after stirring on molecular sieves overnight.[32] The following chemicals were purified by sublimation under high vacuum at 0.17 Torr: DABCO 100 °C then again at 50 °C, potassium *tert*-butoxide 160 °C, *p*-phenylenediamine (**10**) 100 °C, and all stored under a nitrogen atmosphere protected from light.

TLC (Merck Kieselgel silica gel 60 F_{254} aluminium sheets) was used to monitor reaction progress and locate compounds eluted during column chromatography (Grace Davison Discovery Sciences, Davisil silica gel, 60 Å, 40–63 μm). Colourless compounds were visualised by using a UV lamp or permanganate dip stain.

***exo*-Porphyrin Block 4:** A solution of anhydride **2**[13] (168 mg, 1.02 mmol) and aminoporphyrin **3**[14] (646 mg, 1.03 mmol) in degassed $CHCl_3$ (10 mL) was heated to reflux overnight under an argon atmosphere, forming a precipitate. The solvent was removed in vacuo, the residue redissolved in Ac_2O (10 mL), NaOAc (280 mg, 2.06 mmol) added, and the solution heated at 80 °C overnight, after which the Ac_2O was removed by distillation under reduced pressure. The mixture was redissolved in $CHCl_3$ (100 mL), washed with H_2O (2× 100 mL), NaOH (2 M, 3× 100 mL), H_2O (100 mL), dried with Na_2SO_4, filtered, and the solvent removed in vacuo. The crude material was purified by column chromatography (silica, 5% THF/$CHCl_3$), and the solvent removed in vacuo to afford a purple solid (570 mg, 72%), m.p. > 300 °C. ^{1}H NMR (400 MHz, $CDCl_3$, 26 °C, $CHCl_3$): δ = 8.90–8.82 (m, 8 H), 8.32 (d, J = 8.3 Hz, 2 H), 8.22 (dd, J = 1.6, 7.6 Hz, 6 H), 7.82–7.73 (m, 9 H), 7.71 (d, J = 8.3 Hz, 2 H), 6.45 (m, 2 H), 3.56 (s, 2 H), 3.04 (s, 2 H), 1.76 (d, J = 10 Hz, 1 H), 1.71 (d, J = 10 Hz, 1 H), –2.8 (s, 2 H) ppm. HRMS (ESI-TOF-MS): calcd. for $C_{53}H_{38}N_5O_2^+$ [M + H]$^+$ 776.3026; found 776.3044. UV/Vis ($CHCl_3$): λ_{max} (nm) = 418.9, 515.3, 550.5, 589.0, 644.5.

***exo*-Cyclobutene Diester Block 5:** Compound **5** was synthesised by using a modification of the literature procedure[20] although we report different melting point and NMR spectra. A solution of anhydride **2**[13] (8.0 g, 48.7 mmol), DMAD (13.9 g, 2 equiv., 97.5 mmol), and $[RuH_2(CO)(PPh_3)_3]$ (2.24 g, 2.4 mmol, 5 mol-%) in toluene (100 mL) was heated at 100 °C for 3 d under a nitrogen atmosphere and protected from light, forming a precipitate. If precipitation did not occur, the mixture was cooled and hexane added until precipitation occurred. The mixture was filtered, and the precipitate washed with hexane to afford a brown powder (10.0 g, 67%), which was used without further purification. Recrystallised from $CHCl_3$/hexane to afford a beige powder for analysis, m.p. 190–193 °C. ^{1}H NMR (600 MHz, $CDCl_3$, 20 °C, $CHCl_3$): δ = 3.80 (s, 6 H), 2.92 (s, 2 H), 2.90 (d, J = 1.4 Hz, 2 H), 2.89 (s, 2 H), 1.59 (d, J = 12.8 Hz, 1 H), 1.19 (d, J = 12.8 Hz, 1 H) ppm. ^{13}C NMR (150 MHz, $CDCl_3$): δ = 171.89, 160.72, 141.88, 52.40, 47.89, 45.19, 38.70, 27.02 ppm. HRMS (ESI-TOF-MS): calcd. for $C_{15}H_{14}O_7Na^+$ [M + Na]$^+$ 329.0637; found 329.0643.

Porphyrin (*exo*-Cyclobutene Diester Imide) 6: A solution of anhydride **5** (40 mg, 0.13 mmol) and aminoporphyrin **3** (82 mg, 0.13 mmol) in degassed $CHCl_3$ (5 mL) was heated to reflux overnight under an argon atmosphere, forming a precipitate. The solvent was removed in vacuo, and the solids redissolved in Ac_2O (10 mL), NaOAc (100 mg, 0.7 mmol) added, and the solution heated at 80 °C overnight, after which the Ac_2O was removed by distillation under reduced pressure. The mixture was redissolved in $CHCl_3$ (100 mL), washed with H_2O (2× 100 mL), NaOH (2 M, 3× 100 mL), H_2O (100 mL), dried with Na_2SO_4, filtered, and the solvent removed in vacuo. The crude material was purified by column chromatography (silica, 10% THF/$CHCl_3$), the solvent removed in vacuo, and recrystallised from $CDCl_3$/MeOH to afford purple crystals (100 mg, 84%), m.p. (solvent of crystallisation loss 240–245 °C), 262–269 °C. ^{1}H NMR (600 MHz, $CDCl_3$, 20 °C, $CHCl_3$, approximately 1 mM): δ = 8.91–8.81 (m, 8 H), 8.33 (d, J = 8.1 Hz, 2 H), 8.22 (d, J = 7.2 Hz, 6 H), 7.81–7.73 (m, 9 H), 7.70 (d, J = 8.1 Hz, 2 H), 3.86 (s, 6 H), 3.08 (s, 2 H), 3.04 (s, 2 H), 2.95 (s, 2 H), 1.66 (d, J = 12.9 Hz, 1 H), 1.44 (d, J = 12.9 Hz, 1 H), –2.80 (s, 2 H) ppm. HRMS (ESI-TOF-MS): calcd. for $C_{59}H_{44}N_5O_6^+$ [M + H]$^+$ 918.3292; found 918.3313. UV/Vis ($CHCl_3$): λ_{max} (nm) = 418.7, 515.3, 550.7, 589.4, 646.0.

Zn Porphyrin (*exo*-Cyclobutene Diester Imide) 7: Zn metallation of **6** (80 mg, 0.087 mmol) was achieved by using the same procedure as for **1** to afford purple crystals (81 mg, 95%), m.p. (solvent of crystallisation loss 254–255 °C), 272–278 °C. ^{1}H NMR (600 MHz, $CDCl_3$, 20 °C, $CHCl_3$, approximately 5 mM): δ = 8.99–8.93 (m, 8 H), 8.28 (d, J = 8.2 Hz, 2 H), 8.24 (d, J = 6.5 Hz, 6 H), 7.82–7.72 (m, 9 H), 7.48 (d, J = 8.2 Hz, 2 H), 3.84 (s, 6 H), 2.96 (s, 2 H), 2.89 (s, 2 H), 2.72 (s, 2 H), 1.57 (d, J = 12.8 Hz, 1 H), 1.31 (d, J = 12.8 Hz, 1 H) ppm. HRMS (ESI-TOF-MS): calcd. for $C_{59}H_{41}N_5O_6{}^{(64)}ZnNa^+$ [M + Na]$^+$ 1002.2246; found 1002.2280. UV/Vis ($CHCl_3$): λ_{max} (nm) = 419.3, 547.5, 585.0.

***endo*-Cyclobutene Diester Block 9:** Compound **9** was synthesised by using a modification of literature procedure.[20] A solution of anhydride **8**[19] (8.0 g, 48.7 mmol), DMAD[15] (13.9 g, 2 equiv., 97.5 mmol), and $[RuH_2(CO)(PPh_3)_3]$[16] (2.24 g, 2.4 mmol, 5 mol-%) in toluene (100 mL) was heated at 100 °C for 3 d under a nitrogen atmosphere and protected from light, forming a precipitate. The mixture was cooled, filtered, and the precipitate washed with hexane to afford a brown powder (11.6 g, 77%), which was used without further purification. Recrystallised from $CHCl_3$/hexane to afford a white powder for analysis, m.p. 165–167 °C (161–163 °C).[20] ^{1}H NMR (600 MHz, $CDCl_3$, 20 °C, $CHCl_3$): δ = 3.79 (s, 6 H), 3.57–3.52 (m, 2 H), 2.99 (s, 2 H), 2.95–2.89 (m, 2 H), 1.82 (d, J = 11.6 Hz, 1 H), 1.52 (dt, J = 11.6, 1.3 Hz, 1 H) ppm. ^{13}C NMR (100 MHz, $CDCl_3$): δ = 170.78, 160.59, 141.20, 52.33, 48.63, 42.40, 37.36, 34.55 ppm. HRMS (ESI-TOF-MS): calcd. for $C_{15}H_{14}O_7Na^+$ [M + Na]$^+$ 329.0637; found 329.0641.

Linker 11: A solution of **9** (4.92 g, 16.1 mmol) and sublimed *p*-phenylenediamine (**10**, 0.869 g, 8.0 mmol) in dry DMF (80 mL) was heated at 80 °C under an argon atmosphere for 3 d, after which the solution had turned black. The DMF was removed by distillation under reduced pressure, the mixture redissolved in Ac_2O (80 mL), NaOAc (8.75 g, 64.3 mmol) added, and the solution heated at 80 °C under a nitrogen atmosphere for a further 3 d, after which a precipitate sometimes formed. The Ac_2O was removed by distillation under reduced pressure, the mixture redissolved in $CHCl_3$ (200 mL), washed with H_2O (2× 200 mL), NaOH (2 M, 3× 200 mL, or until aqueous phase was no longer black), HCl (2 M, 1× 100 mL), H_2O (1× 100 mL), dried with Na_2SO_4, and the solvent removed in vacuo to afford off-white flakes (1.38 g, 25%), which were used without further purification. Recrystallised from $CHCl_3$/hexane to afford a white powder for analysis, m.p. > 300 °C. ^{1}H NMR (600 MHz, $CDCl_3$, 20 °C, $CHCl_3$): δ = 7.39 (s, 4 H), 3.78 (s, 12 H), 3.43–3.38 (m, 4 H), 2.98 (s, 4 H), 2.97–2.94 (m, 4 H), 1.82 (d, J = 11.4 Hz, 2 H), 1.56 (d, J = 11.4 Hz, 2 H) ppm. ^{13}C NMR (150 MHz, $CDCl_3$): δ = 175.63, 160.73, 141.28, 131.69, 127.22, 52.26, 47.61, 42.62, 36.89, 34.41 ppm. HRMS (ESI-TOF-MS): calcd. for $C_{36}H_{32}N_2O_{12}Na^+$ [M + Na]$^+$ 707.1853; found 707.1832.

Linker Bisepoxide 12: Compound **11** (600 mg, 0.88 mmol) was dissolved in dry CH_2Cl_2 (50 mL) under a nitrogen atmosphere and cooled to 0 °C. Anhydrous *tert*-butyl hydroperoxide in toluene[22] (3.3 M, 664 μL, 2.2 mmol, 2.5 equiv.) was added and stirred for a

further 10 min at 0 °C, after which sublimed potassium *tert*-butoxide (98 mg, 0.88 mmol, 1 equiv.) was added. The mixture was warmed to room temperature over 30 min, during which time a white precipitate formed. After stirring at room temperature for a further 3 h, the mixture was diluted with CH_2Cl_2 (50 mL) and sodium sulfite (10% aqueous solution, 10 mL) added with vigorous stirring for 15 min. The mixture was further diluted with $CHCl_3$ (1 L), washed with brine (500 mL), dried with Na_2SO_4, filtered, and the solvent removed in vacuo, to afford a white powder (237 mg, 28%, 3:1 mixture of **12/11** based on relative NMR integration). Limited solubility in a range of solvents made further purification difficult so **12** was characterised as a mixture with **11**. ^{1}H NMR (400 MHz, $CDCl_3$, 26 °C, $CHCl_3$): δ = as a mixture with **11**, 7.33 (s, 4 H), 3.82 (s, 12 H), 3.44 (s, 4 H), 3.37 (s, 4 H), 2.56 (s, 4 H), 2.2 (d, J = 12 Hz, 2 H), 1.81 (d, J = 12 Hz, 2 H) ppm.

Free Base Tweezer 13: A suspension of **12/11** mixture (0.10 g, 75 mg of **12** based on 3:1 purity, 0.11 mmol) and **4** (0.16 g, 0.21 mmol, 2 equiv. based on **12**) in dry THF (2 mL) was subjected to microwave irradiation. The solvent was removed in vacuo and the material purified by column chromatography (silica, 10% THF/CH_2Cl_2), recovering **4** in the first major porphyrin band, with **13** (88 mg, 38%) eluting as the second major porphyrin band, recrystallised from $CHCl_3$/MeOH to afford purple crystals, m.p. > 300 °C. ^{1}H NMR (600 MHz, $CDCl_3$, 20 °C, $CHCl_3$): δ = 8.84 (s, 16 H), 8.30 (d, J = 8.2 Hz, 4 H), 8.23–8.16 (m, 12 H), 7.81–7.70 (m, 18 H), 7.65 (d, J = 8.2 Hz, 4 H), 7.60 (s, 4 H), 3.98 (s, 12 H), 3.27 (s, 4 H), 2.97 (s, 4 H), 2.89 (s, 4 H), 2.84 (s, 4 H), 2.75 (d, J = 11.1 Hz, 2 H), 2.55 (d, J = 11.9 Hz, 2 H), 2.41 (s, 4 H), 2.34 (s, 4 H), 1.38 (d, J = 11.1 Hz, 2 H), 1.22 (d, J = 11.9 Hz, 2 H), –2.81 (s, 4 H) ppm. HRMS (ESI-TOF-MS): calcd. for $C_{142}H_{107}N_{12}O_{18}^+$ $[M + H]^+$ 2267.7813; found 2267.7854. UV/Vis ($CHCl_3$): λ_{max} (nm) = 419.0, 514.9, 551.1, 590.0, 645.9.

Zn Tweezer 1: A solution of $Zn(OAc)_2{\cdot}2H_2O$ (100 mg, 0.456 mmol) in MeOH (2 mL) was added dropwise down the condenser to a solution of **13** (94 mg, 0.041 mmol) in $CHCl_3$/MeOH (5 mL, 4:1) heated to reflux. The solution was heated to reflux for 15 min, $CHCl_3$ (5 mL) was added, and heated to reflux for a further 15 min. The mixture was cooled, diluted with $CHCl_3$ (100 mL), washed with H_2O, dried with Na_2SO_4, filtered, and the solvent removed in vacuo. The product was purified by column chromatography (silica, 10% THF/$CHCl_3$ to remove minor components at the solvent front, followed by 30% THF/$CHCl_3$), collecting the strong porphyrin band. The solvent was removed in vacuo to afford a purple powder (94 mg, 95%), which was recrystallised from $CHCl_3$/MeOH to afford bright purple crystals for host-guest titrations, m.p. > 300 °C. ^{1}H NMR (600 MHz, $CDCl_3$, 20 °C, $CHCl_3$): δ = 8.96–8.92 (m, 16 H), 8.31 (d, J = 8.3 Hz, 4 H), 8.23–8.18 (m, 12 H), 7.80–7.70 (m, 18 H), 7.66 (d, J = 8.3 Hz, 4 H), 7.60 (m, 4 H), 3.98 (s, 12 H), 3.28 (m, 4 H), 2.97 (s, 4 H), 2.89 (s, 4 H), 2.84 (m, 4 H), 2.76 (d, J = 11 Hz, 2 H), 2.55 (d, J = 12.1 Hz, 2 H), 2.41 (s, 4 H), 2.34 (s, 4 H), 1.39 (d, J = 11 Hz, 2 H), 1.23 (d, J = 12.1 Hz, 2 H) ppm. HRMS (ESI-TOF-MS): calcd. for $C_{142}H_{103}N_{12}O_{18}Zn_2^+$ $[M + H]^+$ 2391.6094; found 2391.6044. UV/Vis ($CHCl_3$): λ_{max} (nm) = 420.1, 548.1, 585.4.

Supporting Information (see footnote on the first page of this article): Characterisation data (^{1}H NMR, ^{13}C NMR, UV/Vis, HRMS) and titration data (UV/Vis, Job Plot).

Acknowledgments

R. B. M. thanks Flinders University for the provision of an Australian Postgraduate Award and the Playford Memorial Trust for a PhD Top-Up Scholarship.

[1] a) M. Hardouin-Lerouge, P. Hudhomme, M. Sallé, *Chem. Soc. Rev.* **2011**, *40*, 30–43; b) P. D. Harvey, C. Stern, C. P. Gros, R. Guilard, *Coord. Chem. Rev.* **2007**, *251*, 401–428; c) J. Leblond, A. Petitjean, *ChemPhysChem* **2011**, *12*, 1043–1051; d) I. Beletskaya, V. S. Tyurin, A. Y. Tsivadze, R. Guilard, C. Stern, *Chem. Rev.* **2009**, *109*, 1659–1713.

[2] a) C.-W. Chen, H. W. Whitlock Jr, *J. Am. Chem. Soc.* **1978**, *100*, 4921–4922; b) S. C. Zimmerman, C. M. VanZyl, *J. Am. Chem. Soc.* **1987**, *109*, 7894–7896; c) J. Leblond, H. Gao, A. Petitjean, J.-C. Leroux, *J. Am. Chem. Soc.* **2010**, *132*, 8544–8545.

[3] C.-H. Lee, H. Yoon, W.-D. Jang, *Chem. Eur. J.* **2009**, *15*, 9972–9976.

[4] a) J. Rebek Jr, J. E. Trend, R. V. Wattley, S. Chakravorti, *J. Am. Chem. Soc.* **1979**, *101*, 4333–4337; b) J. Rebek Jr, R. V. Wattley, *J. Am. Chem. Soc.* **1980**, *102*, 4853–4854; c) J. Rebek Jr, L. Marshall, *J. Am. Chem. Soc.* **1983**, *105*, 6668–6670; d) H.-G. Weinig, R. Krauss, M. Seydack, J. Bendig, U. Koert, *Chem. Eur. J.* **2001**, *7*, 2075–2088; e) H. Yuasa, N. Miyagawa, M. Nakatani, M. Izumi, H. Hashimoto, *Org. Biomol. Chem.* **2004**, *2*, 3548–3556.

[5] a) M. Ayabe, A. Ikeda, S. Shinkai, S. Sakamoto, K. Yamaguchi, *Chem. Commun.* **2002**, 1032–1033; b) D. Sun, F. S. Tham, C. A. Reed, L. Chaker, M. Burgess, P. D. W. Boyd, *J. Am. Chem. Soc.* **2000**, *122*, 10704–10705; c) K. Tashiro, T. Aida, J.-Y. Zheng, K. Kinbara, K. Saigo, S. Sakamoto, K. Yamaguchi, *J. Am. Chem. Soc.* **1999**, *121*, 9477–9478.

[6] a) T. Muraoka, K. Kinbara, T. Aida, *Nature* **2006**, *440*, 512–515; b) J. N. H. Reek, A. P. H. J. Schenning, A. W. Bosman, E. W. Meijer, M. J. Crossley, *Chem. Commun.* **1998**, 11–12; c) P. R. Allen, J. N. H. Reek, A. C. Try, M. J. Crossley, *Tetrahedron: Asymmetry* **1997**, *8*, 1161–1164; d) H. L. Anderson, C. A. Hunter, M. N. Meah, J. K. M. Sanders, *J. Am. Chem. Soc.* **1990**, *112*, 5780–5789; e) P. Ballester, A. I. Oliva, A. Costa, P. M. Deyà, A. Frontera, R. M. Gomila, C. A. Hunter, *J. Am. Chem. Soc.* **2006**, *128*, 5560–5569; f) C. A. Hunter, M. N. Meah, J. K. M. Sanders, *J. Am. Chem. Soc.* **1990**, *112*, 5773–5780; g) P. Ballester, A. Costa, A. M. Castilla, P. M. Deyá, A. Frontera, R. M. Gomilla, C. A. Hunter, *Chem. Eur. J.* **2005**, *11*, 2196–2206; h) L. Baldini, P. Ballester, A. Casnati, R. M. Gomila, C. A. Hunter, F. Sansone, R. Ungaro, *J. Am. Chem. Soc.* **2003**, *125*, 14181–14189; i) J. Etxebarria, A. Vidal-Ferran, P. Ballester, *Chem. Commun.* **2008**, 5939–5941; j) R. Rein, M. Gross, N. Solladié, *Chem. Commun.* **2004**, 1992–1993; k) N. Solladié, N. Aubert, S. Bouatra, C. Bourgogne, F. Bregier, J. Brettar, J.-P. Gisselbrecht, M. Gross, R. Rein, C. Sooambar, V. Troiani, M. Walther, *J. Porphyrins Phthalocyanines* **2003**, *7*, 270–281; l) N. Solladié, S. Bouatra, R. Rein, J. Roeser, *J. Porphyrins Phthalocyanines* **2005**, *9*, 779–787; m) N. Solladié, F. Aziat, S. Bouatra, R. Rein, *J. Porphyrins Phthalocyanines* **2008**, *12*, 1250–1260; n) C. A. Hunter, J. K. M. Sanders, A. J. Stone, *Chem. Phys.* **1989**, *133*, 395–404.

[7] a) S. Gil, M. Palomino-Schätzlein, K. P. Burusco, C. Jaime, A. Virgili, *Chirality* **2010**, *22*, 548–556; b) X. Huang, N. Fujioka, G. Pescitelli, F. E. Koehn, R. T. Williamson, K. Nakanishi, N. Berova, *J. Am. Chem. Soc.* **2002**, *124*, 10320–10335; c) P. Bhyrappa, V. V. Borovkov, Y. Inoue, *Org. Lett.* **2007**, *9*, 433–435; d) V. Borovkov, Y. Inoue, *Eur. J. Org. Chem.* **2009**, 189–197.

[8] J. K. M. Sanders, *The Coordination Chemistry of Oligoporphyrins*, *The Porphyrin Handbook*, Academic Press, **2000**, vol. 3, pp. 347–368.

[9] a) S. P. Gaynor, M. J. Gunter, M. R. Johnston, R. N. Warrener, *Org. Biomol. Chem.* **2006**, *4*, 2253–2266; b) M. R. Johnston, D. M. Lyons, *Supramol. Chem.* **2005**, *17*, 503–511; c) M. R. Johnston, M. J. Latter, R. N. Warrener, *Aust. J. Chem.* **2001**, *54*, 633–636; d) M. R. Johnston, M. J. Gunter, R. N. Warrener, *Chem. Commun.* **1998**, 2739–2740; e) R. N. Warrener, M. R. Johnston, M. J. Gunter, *Synlett* **1998**, 593–595; f) M. R. Johnston, M. J. Latter, R. N. Warrener, *Org. Lett.* **2002**, *4*, 2165–

2168; g) L. Flamigni, G. Marconi, M. R. Johnston, *Phys. Chem. Chem. Phys.* **2001**, *3*, 4488–4494.
[10] a) M. J. Shephard, M. N. Paddon-Row, *J. Phys. Chem. A* **2000**, *104*, 11628–11635; b) D. Margetic, R. N. Warrener, D. N. Butler, D. Officer, *Theor. Chem. Acc.* **2007**, *117*, 239–245; c) J. M. Lawson, A. M. Oliver, D. F. Rothenfluh, Y.-Z. An, G. A. Ellis, M. G. Ranasinghe, S. I. Khan, A. G. Franz, P. S. Ganapathi, M. J. Shephard, M. N. Paddon-Row, Y. Rubin, *J. Org. Chem.* **1996**, *61*, 5032–5054; d) T. D. M. Bell, K. A. Jolliffe, K. P. Ghiggino, A. M. Oliver, M. J. Shephard, S. J. Langford, M. N. Paddon-Row, *J. Am. Chem. Soc.* **2000**, *122*, 10661–10666; e) R. N. Warrener, D. N. Butler, L. Liu, D. Margetic, R. A. Russell, *Chem. Eur. J.* **2001**, *7*, 3406–3414; f) M. J. Gunter, H. Tang, R. N. Warrener, *J. Porphyrins Phthalocyanines* **2002**, *6*, 673–684.
[11] a) Y. Kubo, Y. Murai, J.-i. Yamanaka, S. Tokita, Y. Ishimaru, *Tetrahedron Lett.* **1999**, *40*, 6019–6023; b) M. Kimura, T. Kitamura, M. Sano, T. Muto, K. Hanabusa, H. Shirai, N. Kobayashi, *New J. Chem.* **2000**, *24*, 113–114; c) G. Hungerford, M. Van der Auweraer, J.-C. Chambron, V. Heitz, J.-P. Sauvage, J.-L. Pierre, D. Zurita, *Chem. Eur. J.* **1999**, *5*, 2089–2100; d) S. Anderson, H. L. Anderson, J. K. M. Sanders, *J. Chem. Soc. Perkin Trans. 1* **1995**, 2255–2267; e) R. Beavington, P. L. Burn, *J. Chem. Soc. Perkin Trans. 1* **2000**, 1231–1240; f) S. Yagi, M. Ezoe, I. Yonekura, T. Takagishi, H. Nakazumi, *J. Am. Chem. Soc.* **2003**, *125*, 4068–4069; g) L. H. Tong, J.-L. Wietor, W. Clegg, P. R. Raithby, S. I. Pascu, J. K. M. Sanders, *Chem. Eur. J.* **2008**, *14*, 3035–3044.
[12] a) M. Nakash, J. K. M. Sanders, *J. Org. Chem.* **2000**, *65*, 7266–7271; b) H. L. Anderson, S. Anderson, J. K. M. Sanders, *J. Chem. Soc. Perkin Trans. 1* **1995**, 2231–2245; c) D. Kim, S. Lee, G. Gao, H. S. Kang, J. Ko, *J. Organomet. Chem.* **2009**, *695*, 111–119.
[13] D. Craig, *J. Am. Chem. Soc.* **1951**, *73*, 4889–4892.
[14] R. Luguya, L. Jaquinod, F. R. Fronczek, G. H. Vicente, *Tetrahedron* **2004**, *60*, 2757–2763.
[15] a) T.-a. Mitsudo, K. Kokuryo, T. Shinsugi, Y. Nakagawa, Y. Watanabe, Y. Takegami, *J. Org. Chem.* **1979**, *44*, 4492–4496; b) T.-a. Mitsudo, H. Naruse, T. Kondo, Y. Ozaki, Y. Watanabe, *Angew. Chem.* **1994**, *106*, 595–597; *Angew. Chem. Int. Ed. Engl.* **1994**, *33*, 580–581.
[16] S. D. Robinson, *Inorg. Synth.* **1974**, *15*, 48–50.
[17] J.-H. Fuhrhop, K. M. Smith, *Laboratory methods in porphyrin and metalloporphyrin research*, Elsevier, Amsterdam, New York, **1975**.
[18] The ^{1}H NMR spectrum of **7** was considerably concentration dependent. Resonance shifts of up to 0.2 ppm were observed for the resonances not associated with the porphyrin moiety. This is unexpected because porphyrin aggregation is known to influence the position of β-pyrrole and *meso*-phenyl resonance positions.
[19] O. Diels, K. Alder, *Justus Liebigs Ann. Chem.* **1928**, *460*, 98–122.
[20] M. Shang, R. N. Warrener, D. N. Butler, Y. Murata, D. Margetić, *Mol. Diversity* **2011**, *15*, 541–560.
[21] a) R. N. Warrener, A. C. Schultz, D. N. Butler, S. Wang, I. B. Mahadevan, R. A. Russel, *Chem. Commun.* **1997**, 1023–1024; b) R. N. Warrener, D. N. Butler, D. Margetic, F. M. Pfeffer, R. A. Russell, *Tetrahedron Lett.* **2000**, *41*, 4671–4675.
[22] J. G. Hill, B. E. Rossiter, K. B. Sharpless, *J. Org. Chem.* **1983**, *48*, 3607–3608.
[23] R. C. Foitzik, A. Lowe, F. M. Pfeffer, *Tetrahedron Lett.* **2009**, *50*, 2583–2584.
[24] *Protonic Software*, Leeds, LS150HD, UK (www.hyperquad.co.uk).
[25] a) M. Kasha, H. R. Rawls, M. A. El-Bayoumi, *Pure Appl. Chem.* **1965**, *11*, 371–392; b) A. Osuka, K. Maruyama, *J. Am. Chem. Soc.* **1988**, *110*, 4454–4456.
[26] P. N. Taylor, H. L. Anderson, *J. Am. Chem. Soc.* **1999**, *121*, 11538–11545.
[27] a) H. L. Anderson, *Inorg. Chem.* **1994**, *33*, 972–981; b) C. C. Mak, N. Bampos, J. M. K. Sanders, *Angew. Chem.* **1998**, *110*, 3169–3172; *Angew. Chem. Int. Ed.* **1998**, *37*, 3020–3023.
[28] Owing to the limited solubility of **1** in CD_2Cl_2, the exact stoichiometry of DABCO was approximate. Spectral analysis was complicated by overlap of the *meso*-phenyl signals from **1** and **1**:DABCO. However, no significant broadening of the DABCO or β-pyrrole signals from the complex was observed at –90 °C.
[29] a) J. R. Polam, T. K. Shokhireva, K. Raffii, U. Simonis, F. A. Walker, *Inorg. Chim. Acta* **1997**, *263*, 109–117; b) C. J. Medforth, C. M. Muzzi, K. M. Shea, K. M. Smith, R. J. Abraham, S. Jia, J. A. Shelnutt, *J. Chem. Soc. Perkin Trans. 2* **1997**, 833–837.
[30] This NOESY spectrum also revealed a correlation between an aryl and a norbornyl resonance. This was attributed to the linker phenyl diimide protons and their close proximity to protons in the *endo*-region of the polynorbornyl arm. However, owing to the complexity of the spectra containing signals from both **1** and **1**:DABCO species, no definitive structural information could be gained.
[31] *Spartan '10 for Windows®*, v.1.1.0, Wavefunction, Inc., Irvine, CA, 92612, USA, (http://www.wavefun.com/index.html).
[32] D. D. Perrin, L. Armarego, D. R. Perrin, *Purification of Laboratory Chemicals*, Pergamon Press, Ltd., Oxford, UK, **1966**.

Received: February 7, 2013
Published Online: ■

Molecular Tweezers

Usually molecular tweezers possess a high degree of preorganisation, but we have found that the introduction of several rotational degrees of freedom has little impact on association constant strength.

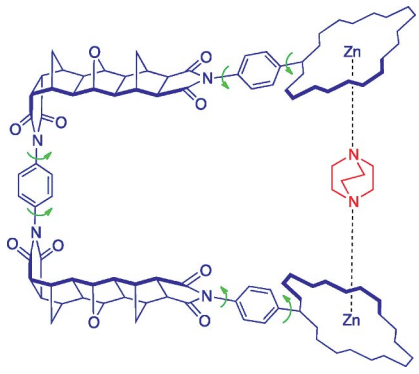

Keywords: Supramolecular chemistry / Molecular recognition / Porphyrinoids / Sandwich complexes / Metalloporphyrins / Cycloaddition

